1521-0111/83/5/949–958$25.00
MOLECULAR PHARMACOLOGY

http://dx.doi.org/10.1124/mol.112.084509
Mol Pharmacol 83:949–958, May 2013

Pharmacology and Structure of Isolated Conformations of the Adenosine A_{2A} Receptor Define Ligand Efficacy[S]

Kirstie A. Bennett, Benjamin Tehan, Guillaume Lebon,[1] Christopher G. Tate, Malcolm Weir, Fiona H. Marshall, and Christopher J. Langmead[2]

Heptares Therapeutics Ltd., Welwyn Garden City, Hertfordshire, United Kingdom (K.A.B., B.T., M.W., F.H.M., C.J.L.); and MRC Laboratory of Molecular Biology, Cambridge, United Kingdom (G.L., C.G.T.)

Received December 18, 2012; accepted February 19, 2013

ABSTRACT

Using isolated receptor conformations crystal structures of the adenosine A_{2A} receptor have been solved in active and inactive states. Studying the change in affinity of ligands at these conformations allowed qualitative prediction of compound efficacy in vitro in a system-independent manner. Agonist 5′-*N*-ethylcarboxamidoadenosine displayed a clear preference to bind to the active state receptor; inverse agonists (xanthine amine congener, ZM241385, SCH58261, and preladenant) bound preferentially to the inactive state, whereas neutral antagonists (theophylline, caffeine, and istradefylline) demonstrated equal affinity for active and inactive states. Ligand docking into the known crystal structures of the A_{2A} receptor rationalized the pharmacology observed; inverse agonists, unlike neutral antagonists, cannot be accommodated within the agonist-binding site of the receptor. The availability of isolated receptor conformations opens the door to the concept of "reverse pharmacology" whereby the functional pharmacology of ligands can be characterized in a system-independent manner by their affinity for a pair (or set) of G protein–coupled receptor conformations.

Introduction

The G protein-coupled receptor (GPCR) super-family comprises ~800 proteins that respond to a variety of ligands to create intracellular responses via G proteins, β-arrestins, and other downstream effectors. GPCRs are important therapeutic targets; over 26% of all Food and Drug Administration (FDA)-approved drugs act at rhodopsin-like GPCRs (Overington et al., 2006). The adenosine A_{2A} receptor is one of four adenosine receptor subtypes (A_1, A_{2A}, A_{2B}, and A_3) belonging to the class A GPCR family (Foord et al., 2005) and activated by adenosine, released in response to ischemic or metabolic stress (Fredholm et al., 2011). A_{2A} receptor agonists have been in clinical trials for treatment of glaucoma and inflammatory diseases (www.clinicaltrials.gov), whereas A_{2A} receptor antagonists/inverse agonists, exemplified by preladenant and istradefylline, have shown promise as a nondopaminergic approach to the treatment of Parkinson's disease (Pinna, 2009).

Designing specific compounds with drug-like properties for GPCRs has been hampered by lack of structural information about activation mechanisms and binding sites. Obtaining high-resolution structures of GPCRs has been complicated by intrinsic protein flexibility and instability in detergent. Recent technological breakthroughs have led to the publication of several GPCR structures, including β adrenergic, histamine, and adenosine A_{2A} receptors (for a review, see Katritch et al., 2012).

One method used to aid structure determination is the stabilized receptor (StaR) method (Warne et al., 2008; Shibata et al., 2009; Robertson et al., 2011), where GPCRs are made stable in short-chain detergent by the introduction of a small number of point mutations in transmembrane (TM) domains but outside known ligand-binding domains. These mutations increase thermostability of the receptor by locking it in a particular conformation (i.e., inactive or active), directed by the pharmacology of the ligand used during the protein engineering process (Robertson et al., 2011; Tate and Schertler, 2009). Using the StaR method, active-state (GL0, GL23, GL26, and GL31) and inactive-state (StaR2) adenosine A_{2A} StaRs have been engineered, allowing solving of crystal structures of agonist-bound and inverse agonist-bound adenosine A_{2A} receptors (Dore et al., 2011; Lebon et al., 2011b). Recently,

[1]Current affiliation: Institut de Génomique Fonctionnelle, Montpellier, France.
[2]Current affiliation: Monash Institute of Pharmaceutical Sciences, Monash University, Melbourne, Victoria, Australia.
dx.doi.org/10.1124/mol.112.084509.
[S] This article has supplemental material available at molpharm.aspetjournals.org.

ABBREVIATIONS: ANOVA, analysis of variance; ATL146e, (4-(3-[6-amino-9-(5-ethylcarbamoyl-3,4-dihydroxy-tetrahydro-furan-2-yl)-9H-purin-2-yl]-prop-2-ynyl)-cyclohexanecarboxylic acid methyl ester); BPM, biophysical mapping; CGS15941, (9-chloro-2-(furan-2-yl)-[1,2,4]triazolo[1,5-c]quinazolin-5-amine); CGS21680, (2-p-(2-carboxyethyl)phenethylamino-5'-N- ethylcarboxamidoadenosine); CHO, Chinese hamster ovary; GPCR, G protein-coupled receptor; NECA, 5′-*N*-ethylcarboxamidoadenosine; Ro 20-1724, (4-(3-Butoxy-4-methoxybenzyl)imidazolidin-2-one); SCH58261, (5-Amino-7-(2-phenylethyl)-2-(2-furyl)-pyrazolo(4,3-e)-1,2,4-triazolo(1,5-c)pyrimidine); SDM, site-directed mutagenesis; StaR, stabilized receptor; TM, transmembrane; XAC, xanthine amine congener 8-[4-[[[[(2-aminoethyl)amino]carbonyl]methyl]oxy]phenyl]-l,3-dipropylxanthine; ZM241385, 4-(2-[7-amino-2-(2-furyl)[1,2,4]triazolo[2,3-*a*][1,3,5]triazin-5-ylamino]ethyl)phenol.

the benefit of structure-based drug design has been demonstrated at GPCRs with the adenosine A_{2A} crystal structure used to aid discovery of a novel chemical series of receptor antagonists (Congreve et al., 2012; Langmead et al., 2012).

Many models have been developed to describe receptor activation (for examples, see De Lean et al., 1980; Samama et al., 1993), the simplest of which is the two-state model (Fig. 1; Leff, 1995) that describes receptors existing in active (R*) or inactive (R) forms. The equilibrium between R and R* is defined by the isomerization constant 'L' (L=R*/R). Although the two-state model does not account for such phenomena as biased agonism or multiple conformations that exist between R and R* (see Perez et al., 1996), the model is extremely useful conceptually, describing interactions of many GPCR ligands. Agonists are described to bind with higher affinity to R*, inverse agonist to R, whereas neutral antagonists bind with equal affinity to R and R*.

At the inactive-state A_{2A} StaR, there is a significant decrease in the affinity of agonists [CGS21680 (2-p-(2-carboxyethyl) phenethylamino-5′-N- ethylcarboxamidoadenosine) and 5′-*N*-ethylcarboxamidoadenosine (NECA)] at the receptor with a corresponding slight increase in inverse agonist affinity (Robertson et al., 2011). Agonist affinity at a receptor fully locked into the R* conformation is expected to be increased compared with that at a wild-type receptor (as demonstrated at a constitutively active mutant of the β2 adrenoreceptor; Samama et al., 1993). At the active-state adenosine A_{2A} receptor constructs, the affinity of such agonists as NECA, CGS21680, and ATL146e (4-(3-[6-amino-9-(5-ethylcarbamoyl-3,4-dihydroxy-tetrahydro-furan-2-yl)-9H-purin-2-yl]-prop-2-ynyl)-cyclohexanecarboxylic acid methyl ester) is unaltered compared with the wild-type, although there is significant decrease in inverse agonist affinity (Lebon et al., 2011a), suggesting the receptor is stabilized in a conformation toward the fully active state.

Although previous studies have shown correlation between the ratio of the dissociation constants of agonists at low(R): high(R*) affinity states and efficacy (e.g., at the β-adrenoceptors; Kent et al., 1980), these studies rely on the use of saturating concentrations of guanyl nucleotides to eliminate high-affinity binding sites. For some receptors, it is difficult to see the difference in agonist affinities for R* and R; indeed, for the A_{2A} receptor, NECA binding appears insensitive to GTP (Guo et al., 2012).

Here we show that measuring changes in ligand-binding affinity at isolated active and inactive A_{2A} receptor states can be used to predict and interpret findings from functional assays in a system-independent manner. Furthermore, we demonstrate that ligand docking into active and inactive-state crystal structures supports the pharmacology and demonstrates the importance of receptor conformation in crystal structure determination and drug design.

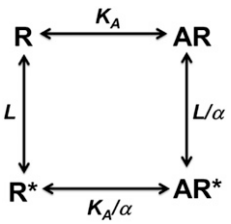

Fig. 1. Two-state model of GPCR activation. A receptor can exist in an inactive (R) or active (R*) form. An inactive receptor may isomerize to the active form (R*) even in the absence of an agonist, a property known as constitutive activity. Once the ligand is bound, the receptor can exist in two states, occupied (AR) or occupied and activated (AR*), the latter being the species that couples to G protein (Strange, 2000). The position of equilibrium between R and R* will depend on the isomerization constant (*L*), the conformational change that takes place. An inverse agonist will bind stronger to R keeping the receptor in the inactive state (form AR), whereas an agonist will bind stronger to R* pushing the equilibrium toward AR*. K_A and K_A/α are the equilibrium constants for agonist binding to the receptor conformations R and R*, respectively; α defines the efficacy of A.

Materials and Methods

Materials. Adenosine deaminase, GeneJuice, and hygromycin B were purchased from Merck Biosciences Ltd (Nottingham, UK). Blasticidin S hydrochloride and doxycycline hydrochloride were purchased from Apollo Scientific (Cheshire, UK). NECA, SCH58261 (5-Amino-7-(2-phenylethyl)-2-(2-furyl)-pyrazolo(4,3-e)-1,2,4-triazolo(1, 5-c)pyrimidine), TryplE, and xanthine amine congener 8-[4-[[[[(2-aminoethyl)amino]carbonyl]methyl]oxy]phenyl]-l,3-dipropylxanthine (XAC) were purchased from Sigma-Aldrich (Gillingham, Kent). CGS15943 (9-chloro-2-(furan-2-yl)-[1,2,4]triazolo[1,5-c]quinazolin-5-amine), CGS21680, Ro 20-1724 (4-(3-Butoxy-4-methoxybenzyl)imidazolidin-2-one), and ZM241385 ((4-(2-[7-amino-2-(2 -furyl) [1,2,4]-triazolo[2, 3-a][1,3,5]triazin- 5-yl amino]ethyl) phenol)) were purchased from Tocris Biosciences (Bristol, UK). Preladenant and istradefylline was synthesized in-house. All other chemicals were obtained from standard commercial sources.

Receptor Constructs. Wild-type receptor pharmacology was explored both at the full-length adenosine A_{2A} receptor (accession number NM_000675) and at a C-terminally truncated version, $A_{2A(1\text{-}316)}$. The C-terminal tail of the A_{2A} receptor was removed from all of the inactive ($StaR2_{(1\text{-}316)}$; Dore et al., 2011; Robertson et al., 2011) or active ($GL0_{(1\text{-}316)}$, $GL23_{(1\text{-}316)}$, $GL26_{(1\text{-}316)}$ and $GL31_{(1\text{-}316)}$; Lebon et al., 2011b) StaRs to aid receptor crystallization. In addition, full-length versions of GL0, GL23, GL26, and GL31 were engineered and used in this study. Constructs and mutations are summarized in Supplemental Table 1.

Maintenance and Transfection of Chinese Hamster Ovary Cells. Chinese hamster ovary (CHO) cells were maintained in culture in Dulbecco's modified Eagle's medium-Hams F-12 media containing 10% fetal calf serum (v/v) and 1% penicillin/streptomycin mixture at 37°C in a humidified air/5% CO_2 atmosphere. Cells were passaged three times a week using TryplE. Using GeneJuice per manufacturer's instructions, 70% confluent cells were transfected with receptor construct (in pcDNA3). Membranes were prepared from CHO cells 48 hours after transfection. T-REx CHO cells (Life Technologies, Paisley, UK) were maintained in Dulbecco's modified Eagle's medium-Hams F-12 mixture supplemented with 10% (v/v) tetracycline-free fetal calf serum, 1% penicillin/streptomycin mixture, and 10 μg/ml blasticidin S hydrochloride at 37°C in a humidified air/5% CO_2 atmosphere.

Generation of a Stable Adenosine $A_{2A(1\text{-}316)}$ Receptor Cell Line. T-REx CHO cells were transfected with pcDNA5/TO from Life Technologies Ltd (Paisley, UK), containing $A_{2A(1\text{-}316)}$ using GeneJuice (as per manufacturer's instructions). After 48 hours, media were replaced with medium-supplemented 200 μg/ml hygromycin B to select for stably expressing clones. Single colonies were selected and grown in media supplemented with doxycycline (1 μg/ml; 16 hours) before being screened for receptor expression using a cAMP accumulation assay.

Radioligand Binding Assays. Cells were harvested and membranes prepared as previously described (Robertson et al., 2011). Radioligand binding assays were carried out using membranes prepared from CHO cells transiently expressing A_{2A}, $A_{2A\ (1\text{-}316)}$, the active state (GL0, GL23, GL26, and GL31) or inactive state

($StaR2_{(1-316)}$) StaRs. Due to low affinity of [^{3}H]NECA at $StaR2_{(1-316)}$, affinity measurements for this construct were made using [^{3}H]ZM241385 competition binding assays. Membranes (5 μg) expressing the wild type or $StaR2_{(1-316)}$ were incubated with 2 nM [^{3}H]ZM241385 (50 Ci/mmol; American Radiolabeled Chemicals, Inc., St. Louis, MO) in the presence or absence of competing compounds with 1 μM CGS15943 used to define nonspecific binding. After a 90-minute incubation at room temperature, assays were terminated by rapid filtration through 96-well GF/B filter plates presoaked with 0.1% polyethyleneimine using a 96-well head harvester (Tomtec, Hamden, CT) and plates washed with 5 $\times$ 0.5 ml water. Plates were dried, and bound radioactivity was measured using scintillation spectroscopy on a Microbeta counter (PerkinElmer, Waltham, MA). [^{3}H]NECA (15.9 Ci/mmol; PerkinElmer) competition and saturation binding assays were carried out as previously described (Lebon et al., 2011b). Membranes (10–15 μg/well) from cells expressing at wild-type or active-state StaRs were assessed using [^{3}H]NECA binding in buffer containing 50 mM Tris–HCl (pH 7.4). Nonspecific binding was defined using 1 μM CGS21680. After a 1-hour incubation at 25°C, plates were harvested and read as previously described.

cAMP Accumulation Assay. Cells were seeded at a density of 25,000 cells/well in 96-well half area plates, and receptor expression was induced with the inclusion of 0, 0.3, or 10 ng/ml doxycycline in the media. After 16 hours, media were removed from the cells and replaced with 25 μl Kreb's media containing 2 U/ml adenosine deaminase in the absence or presence of ligand. Cells were incubated at 37°C for 30 minutes prior to addition of 25 μl Krebs media supplemented with the phosphodiesterase inhibitor, Ro 20-1724 (100 μM, 25°C, 30 minutes). Cells were then lysed, and any cAMP produced was detected using the dynamic 2 cAMP HTRF kit (CisBio International, Avignon, France) according to manufacturer's instructions before plates were read on a PheraStar fluorescence plate reader (BMG LabTech, Ortenberg, Germany).

Data Analysis. Data were analyzed using GraphPad Prism version 5.0 (GraphPad Software, San Diego, CA). Inhibition-binding curves were fitted to a four-parameter logistic equation to determine IC_{50} values, which were converted into K_i values using K_D values determined by saturation binding and the radioligand concentration ([^{3}H]NECA ~10 nM; [^{3}H]ZM241385 ~2 nM). Functional concentration-response data were fitted to a three-parameter logistic equation. Statistical tests used in this study included unpaired, two-tailed t tests to compare two data sets ($\alpha = 0.05$) and one-way analysis of variance (ANOVA) (with Dunnett's post-hoc test if $P < 0.05$) to analyze multiple data sets ($\alpha = 0.05$).

Molecular Modeling and Ligand Docking. The alignment of the inactive state crystal structures of the adenosine A_{2A} receptor in complex with ZM241385 (3PWH), XAC (3REY), and caffeine (3RFM), onto the activated form of the receptor in complex with NECA (2YDV), was performed using the align algorithm within PyMOL (The PyMOL Molecular Graphics System, version 1.3; Schrödinger, LLC, New York, NY). The binding cavity within 2YDV was generated within PyMOL from an apo version of the protein using the "Cavities and Pockets (Culled)" detection algorithm with default values for Cavity Detection Radius and Cutoff.

The ligand docking experiments were guided by ligand structure activity relationship and by our iterative process of assessing literature site-directed mutagenesis (SDM) and then designing and testing our own mutants using biophysical mapping (BPM; Zhukov et al., 2011) to identify possible binding modes. The protein preparation and docking experiments were done within the Schrödinger Maestro package (Maestro, version 9.2; Schrödinger, LLC) utilizing the structure of the inactive adenosine A_{2A} receptor (3PWH), as the basis for subsequent dockings. The grid generation necessary for docking was done within Glide. The residues highlighted in previous BPM experiments (Zhukov et al., 2011) were used to define the cavity of the grid; however, no constraints were added in the grid generation to ensure that subsequent dockings were not biased in any way. Glide XP docking was carried out on all of the ligands in question with 10 poses per ligand being stored. The poses were then assessed against the BPM data and the best solution identified.

Results

Agonist Binding to the Active-State Adenosine A_{2A} Receptor. To test for changes in agonist affinity at the active-state StaRs, saturation binding experiments were performed using the radiolabeled agonist [^{3}H]NECA. The radiolabeled agonist bound with high affinity to the wild-type adenosine A_{2A} receptor ($pK_D = 8.22 \pm 0.16$); there was no significant change in the affinity of [^{3}H]NECA for the active state constructs (GL0, GL23, GL26, and GL31) compared with the wild-type A_{2A} receptor ($P = 0.28$; one-way ANOVA; Supplemental Table 2), nor was there any significant change in the affinity of [^{3}H]NECA between the full-length (A_{2A}) and C-terminally truncated [$A_{2A(1-316)}$] receptor ($P = 0.51$; unpaired two-tailed t test; Supplemental Table 2). A trend could be seen where an increase in receptor thermostability led to an increase in receptor expression (B_{max}), with GL26 and GL31 exhibiting significantly higher receptor expression levels compared with wild-type ($P < 0.01$ A_{2A} versus GL26 and $P < 0.05$ A_{2A} versus GL31; as measured using a one-way ANOVA with Dunnett's post-hoc test; Supplemental Table 2). The truncated $A_{2A(1-316)}$ receptor was expressed at significantly higher expression levels than the full-length A_{2A} receptor ($P = 0.01$; unpaired two-tailed t test; Supplemental Table 2).

Differential Changes in "Antagonist" Affinities at Isolated Receptor Conformations. To test whether affinity was altered at the active-state StaRs, a panel of "antagonist" affinities were measured in [^{3}H]NECA competition-binding assays. There was a significant decrease in affinity of preladenant, SCH58261, XAC, and ZM241385 at the active-state StaRs compared with the wild-type A_{2A} receptor ($P < 0.05 < 0.001$; one-way ANOVA with Dunnett's post hoc-test; Fig. 2; Table 1), although the affinities of caffeine, istradefylline, and theophylline were not significantly altered ($P > 0.05$; one-way ANOVA; Fig. 2; Table 1). There was a trend for the affinity of unlabeled NECA to increase at the active state StaRs, although this was only significant at two of the active-state constructs (GL0 and GL31; $P < 0.01$, one-way ANOVA with Dunnett's post-hoc test).

In contrast to active-state StaRs, agonist affinity is decreased at receptors stabilized into the inactive conformation, whereas antagonist/inverse agonist affinity is maintained (or even increased; Dore et al., 2011; Robertson et al., 2011). As the inactive-state construct, $StaR2_{(1-316)}$, has previously been shown to have very low affinity for NECA (Dore et al., 2011); therefore, an inverse agonist radioligand ([^{3}H]ZM241385) was used to determine the affinity of ligands at $StaR2_{(1-316)}$. The affinity of NECA, theophylline, istradefylline, XAC, and SCH58261 at $A_{2A(1-316)}$ were similar when measured using [^{3}H]NECA compared with affinities measured using [^{3}H]ZM241385 (Robertson et al., 2011; Supplemental Table 3). Previous studies have suggested that the high-affinity state of the recombinant human A_{2A} is not easily observed when receptor is expressed in HEK293 cells (Rieger et al., 2001; Sullivan et al., 2001), possibly due to low levels of $G_{\alpha s}$ in these cell lines relative to the expression of the receptor. This may explain why affinities of agonists, neutral antagonists, and inverse agonists are similar at $A_{2A(1-316)}$ when affinity is measured using agonist and inverse agonist radioligands.

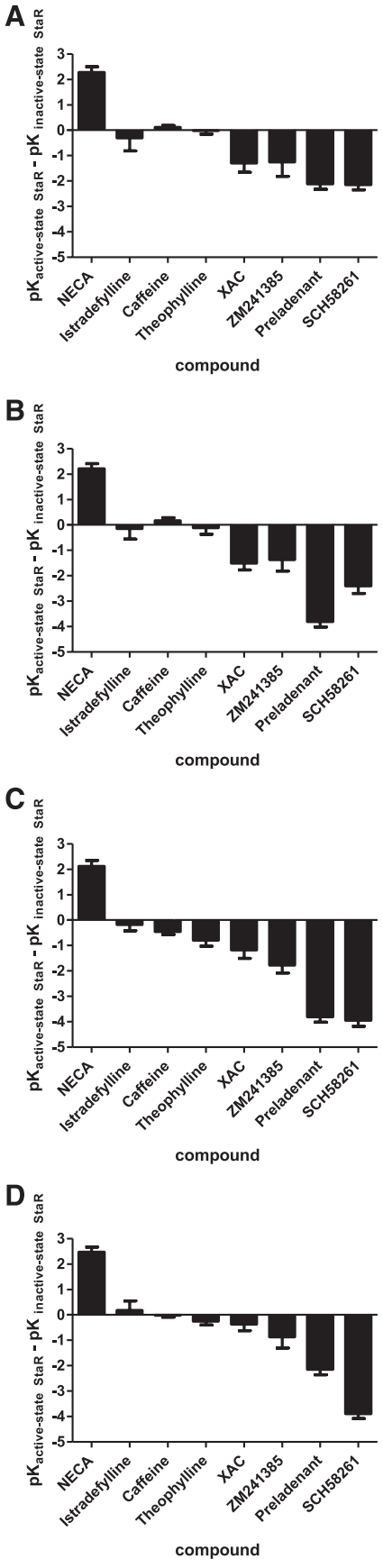

Fig. 2. Differences in affinity of agonist (NECA) or "antagonists" (ZM241385, XAC, istradefylline, SCH58261, preladenant, theophylline, and caffeine) at the active and inactive state StaRs. Data from Table 1 has been displayed as change (± S.E.M.) in pK_i of active-state StaR (pK_i StaR minus pK_i A_{2A}) compared with inactive-state StaR [pK_i $StaR2_{(1\text{-}316)}$ minus pK_i $A_{2A(1\text{-}316)}$] for (A) GL0, (B) GL23, (C) GL26, and (D) GL31.

Saturation binding experiments demonstrated the pK_D ± S.E.M. of [^{3}H]ZM241385 at $StaR2_{(1\text{-}316)}$ to be 8.72 ± 0.1, in good agreement with previous reported measures. However, NECA showed a dramatic reduction in affinity at $StaR2_{(1\text{-}316)}$ compared with wild-type $A_{2A(1\text{-}316)}$ (Table 1; $P < 0.01$; unpaired two-tailed t test), whereas the affinity of ZM241385, XAC, SCH58261, and preladenant remained unaltered (Table 1; $P = 0.86$; $P = 0.44$; $P = 0.07$; $P = 0.38$, respectively; unpaired two-tailed t test). Interestingly, theophylline and caffeine showed slightly decreased affinities at $StaR2_{(1\text{-}316)}$ ($P < 0.05$ for theophylline, and $P < 0.05$ for caffeine; unpaired two-tailed t test), whereas the affinity of istradefylline remained unaltered at both agonist and inverse agonist ($StaR2_{(1\text{-}316)}$) constructs ($P = 0.39$).

The affinity data from Table 1 was plotted as change in pK_i of active-state StaRs (pK_i StaR minus pK_i A_{2A}) compared with inactive-state StaR (pK_i $StaR2_{(1\text{-}316)}$ minus pK_i $A_{2A(1\text{-}316)}$) to indicate the affinity differential between the two isolated conformations (Fig. 2). When compared with each of the active-state constructs (GL0, GL23, GL26 and GL31), preladenant and SCH58261 were shown to display a strong preference for the inactive state of the adenosine A_{2A} receptor. The magnitude of this preference was even greater than that for ZM241385, even though ZM241385 has higher affinity for the wild-type receptor. On the other hand, istradefylline, caffeine, and theophylline show little preference in binding to either the active or inactive receptor states, as evidenced by log ratios close to zero (Fig. 2).

Differential Functional Pharmacology of Adenosine A_{2A} Receptor "Antagonists.". To assess the predictions made by binding of adenosine A_{2A} receptor ligands to isolated receptor conformations, a cAMP accumulation assay was used to measure receptor responses through the $G_{\alpha s}$ pathway. To allow a degree of control in receptor expression levels within experiments T-Rex-CHO-A_{2A} and T-Rex-CHO-$A_{2A(1\text{-}316)}$ cells lines were created placing receptor expression under the control of the tetracycline receptor/operator system (addition of tetracycline or doxycycline to the media induces receptor expression). Both T-Rex-CHO-A_{2A} and T-Rex-CHO-$A_{2A(1\text{-}316)}$ cells lines showed constitutive receptor activity, allowing measurements of ligands that increase (agonists) or decrease (inverse agonists) receptor activity. After some optimization, the $A_{2A(1\text{-}316)}$ cell line was shown to respond better to agonist and inverse agonists because there was a larger response signal (Bennett et al., 2011); because agonist and inverse agonist affinities were not significantly different at $A_{2A(1\text{-}316)}$ compared with A_{2A} (Supplemental Table 2; Table 1), the T-Rex-CHO-$A_{2A(1\text{-}316)}$ cell line was used for all functional studies.

Initial studies were carried out to establish ligand pharmacology under different levels of receptor induction (and hence expression and constitutive activity). Over a range of doxycycline concentrations (0–10 ng/ml), basal cAMP levels could be titrated such that a range of responses could be observed. Receptor expression levels at each of the doxycycline concentrations were measured using a [^{3}H]NECA binding assay; it appeared that very low receptor expression levels were needed to detect functional effects as receptor

TABLE 1

Affinity of a panel of compounds at wild-type, active-state, and inactive-state StaRs as measured by competition radioligand binding

An unpaired, two-tailed t test was used to compare affinity of compounds at A_{2A} and $A_{2A(1-316)}$; there was no significant difference at any compound tested ($P > 0.05$). By comparing affinity of compounds at $StaR2_{(1-316)}$ and $A_{2A(1-316)}$ with an unpaired two-tailed t test, it was revealed that NECA had a significantly reduced affinity at $StaR2_{(1-316)}$. All data were generated using [^{3}H]NECA as the radioligand, except for $StaR2_{(1-316)}$ where [^{3}H]ZM241385 was used due to the low affinity of agonists for this construct. pKi displayed as mean ± S.E.M. of n = 3–5.

	Wild Type		Active State				Inactive State
	A_{2A}	$A_{2A(1-316)}$	GL0	GL23	GL26	GL31	$StaR2_{(1-316)}$
NECA	8.14 ± 0.20	7.82 ± 0.20	8.67 ± 0.10**	8.60 ± 0.05	8.51 ± 0.13	8.86 ± 0.04**	6.07 ± 0.20††
Caffeine	5.44 ± 0.15	5.78 ± 0.18	4.97 ± 0.54	5.02 ± 0.42	4.40 ± 0.25	4.83 ± 0.40	5.19 ± 0.16†
Istradefylline	7.42 ± 0.14	7.12 ± 0.14	7.38 ± 0.26	7.54 ± 0.10	7.50 ± 0.24	7.86 ± 0.08	7.38 ± 0.24
Theophylline	5.74 ± 0.09	5.94 ± 0.14	5.15 ± 0.49	5.05 ± 0.39	4.37 ± 0.19	4.91 ± 0.34	5.36 ± 0.15†
ZM241385	9.17 ± 0.23	9.22 ± 0.04	7.30 ± 0.03***	7.18 ± 0.24***	6.77 ± 0.15***	7.68 ± 0.02***	8.60 ± 0.19
XAC	8.41 ± 0.47	8.56 ± 0.04	6.93 ± 0.05***	6.72 ± 0.01***	7.06 ± 0.04***	7.86 ± 0.02*	8.38 ± 0.21
SCH58261	8.89 ± 0.19	8.86 ± 0.13	6.30 ± 0.09***	6.05 ± 0.23***	4.51 ± 0.21***	4.56 ± 0.08***	8.42 ± 0.12
Preladenant	8.95 ± 0.06	8.76 ± 0.12	6.33 ± 0.05***	4.63 ± 0.10***	4.63 ± 0.10***	6.29 ± 0.04***	8.63 ± 0.05

* $P < 0.05$; *** $P < 0.001$, when comparing affinity at active state receptors to A_{2A} (one-way ANOVA with Dunnett's post-hoc test).
† $P < 0.05$; †† $P < 0.01$.

expression could only be detected at high (10 ng/ml) doxycycline levels (0.29 ± 0.03 pmol/mg). Due to a degree of system-leakiness, it was possible in basal conditions (0 ng/ml doxycycline) to achieve assay conditions where there was little or no constitutive activity and a full NECA response could be seen; however, there was no window for inverse agonism to be detected (Fig. 3A). In contrast, when fully induced with a high concentration of doxycycline (10 ng/ml), it was possible to elevate the basal level of cAMP to such a level that no further NECA response could be observed, although inverse agonism could be detected (Fig. 3C). Using a doxycycline concentration of 0.3 ng/ml, it was possible to achieve an intermediate level of constitutive activity to enable the detection of both positive and inverse agonism (Fig. 3B; Supplemental Table 4). Thus, only using a very specifically designed functional assay is it possible to functionally delineate the pharmacology of inverse agonists and either partial inverse agonists or neutral antagonists.

Cells were challenged with NECA, causing a concentration-dependent increase in cAMP accumulation levels (Fig. 4A). Incubating cells with preladenant decreased cAMP levels in a concentration-dependent manner to the level seen in the absence of doxycycline-induced receptor expression, except at high doxycycline concentrations where preladenant appeared to act as a partial inverse agonist (Fig. 4B). Theophylline appeared to have no effect on cAMP accumulation levels at all doxycycline concentrations tested, indicating neutral antagonism (Fig. 4C). Istradefylline and caffeine, which showed little preference in binding to active and inactive state receptor constructs (Fig. 2; Table 1), also appeared to act as neutral antagonists (Supplemental Fig. 1, A and B). In contrast, ZM241385, SCH58261, and XAC showed a preference to binding to the inactive state receptor constructs and acted as inverse agonists (Supplemental Fig. 1, C–E). These observations appear to be concordant with the binding affinities for the active and inactive conformations of the receptor.

Active and Inactive State Crystal Structures Infer Differences in Binding Pockets to Explain Ligand Pharmacology. Crystal structures have been determined for the adenosine A_{2A} receptor in both an active state (in complex with adenosine or NECA; Lebon et al., 2011b) and an inactive state (in complex with ZM241385, XAC, and caffeine; Dore et al., 2011). To aid the interpretation of the results from binding and functional assays, a comparison between ligand-binding sites in active and inactive conformations was made.

Figure 5A shows the structure of the NECA-bound adenosine A_{2A} receptor (Protein Data Bank code: 2YDV). Residues that are thought to be important in changes between ground state and the agonist-bound or activated state are highlighted ($H278^{7.43}$, $S277^{7.42}$ and $N253^{6.55}$). Agonist binding to the receptor appears to result in a rotameric change in $H278^{7.43}$ and inwards movement of TM domains 1, 5, and 7 and upwards movement of TM domain 3, resulting in a significant contraction in the volume of the binding site. In Fig. 5, the extent of the agonist state receptor binding pocket is highlighted in gray (only TM1 is shown for clarity). Overlay analysis shows that the surface of the NECA binding site is not significantly different in the key regions of interest to that of the agonist UK-432097-bound adenosine A_{2A} receptor (Supplemental Fig. 2).

The crystal structures of inactive-state adenosine A_{2A} receptors are shown in Figs. 5B and 6B overlaid onto the NECA-bound structure. ZM241385 and XAC bind perpendicular to the membrane, however, it is clear that the inverse agonists ZM241385 (3PWH; Fig. 5B) and XAC (3REY; Fig. 5C) would not be accommodated in the binding site of active-state A_{2A} receptor, as shown by their protruding beyond the surface displayed in gray. More subtly, ZM241385 sterically prevents the ~2Å inward movement of $H250^{6.52}$, which is thought to accompany receptor activation as a result of the inward "bulge" of TM5 (Lebon et al., 2011b; Supplemental Fig. 3).

In contrast, the neutral antagonist caffeine, a small fragment-sized molecule, appears to dock equally well into the binding site of the active state A_{2A} receptor structure (in a position similar to the xanthine portion of XAC), suggesting that binding of caffeine does not sterically preclude the adenosine A_{2A} receptor from adopting an active state when bound (Fig. 5D).

It is worth noting that in all active state StaRs, the stabilizing mutations are outside the ligand-binding domain, meaning that no mutations are within 5Å of the binding site of the ligands tested in this study. In the inactive state StaR, two mutations are near the active site; the $S277^{7.42}$A mutation is within the ribose-binding pocket, and $T88^{3.36}$A is on TM3 where NECA has been shown to interact within the active-state receptor. It has previously been shown (by back-mutating these residues on the inactive state StaR; see Supplementary Table 2 in Dore et al., 2011) that $S277^{7.42}$A and $T88^{3.36}$A mutations do not affect affinity of agonists at the inactive state StaR.

On the basis of previous SDM data (Zhukov et al., 2011) and of binding and functional data, the clinically evaluated

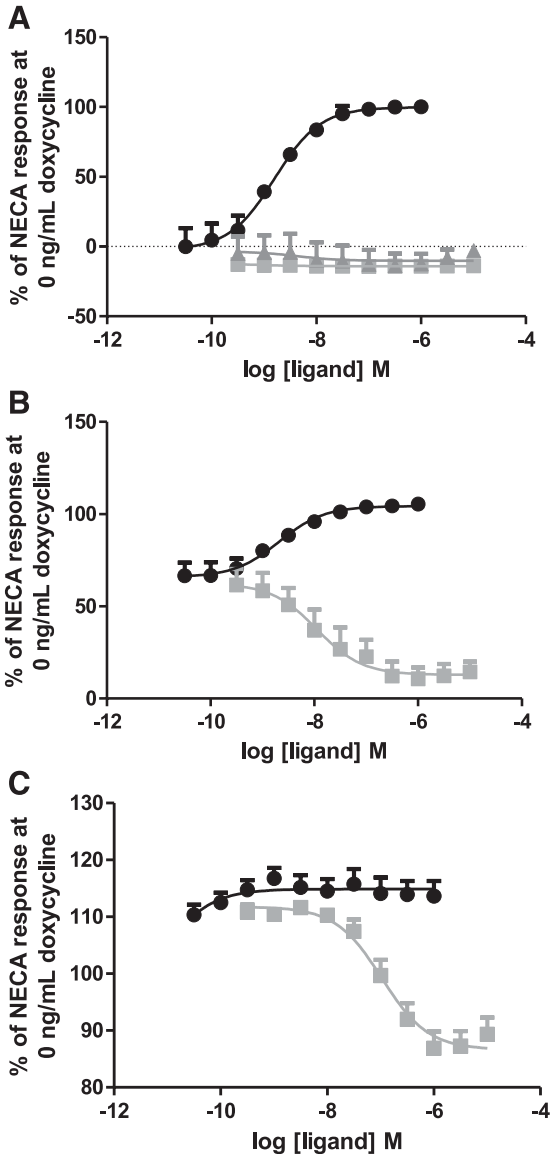

Fig. 3. Titration of adenosine A_{2A} receptor constitutive activity by changes in receptor expression. Response of the adenosine $A_{2A(1-316)}$ receptor in functional assays is system-dependent. (A) In the absence of doxycycline, there is a good "window" to see agonist (NECA; filled circle) responses, although the system cannot detect the difference in inverse agonist (SCH58261; filled square) and neutral antagonist (istradefylline; filled triangle) responses. (B) At high levels of receptor expression (10 ng/ml doxycycline), constitutive activity levels have reached the system maximal response level; therefore, no further increase in response is seen after challenge by NECA (filled circle), although there is a clear inverse agonist response by SCH58261 (filled square). (C) At 3 ng/ml doxycycline, receptor expression levels are such to differentiate between agonist (NECA; filled tlsb .01wcircle) and inverse agonist (SCH58261; filled square) responses. Data plotted as mean ± S.E.M. of $n = 3$.

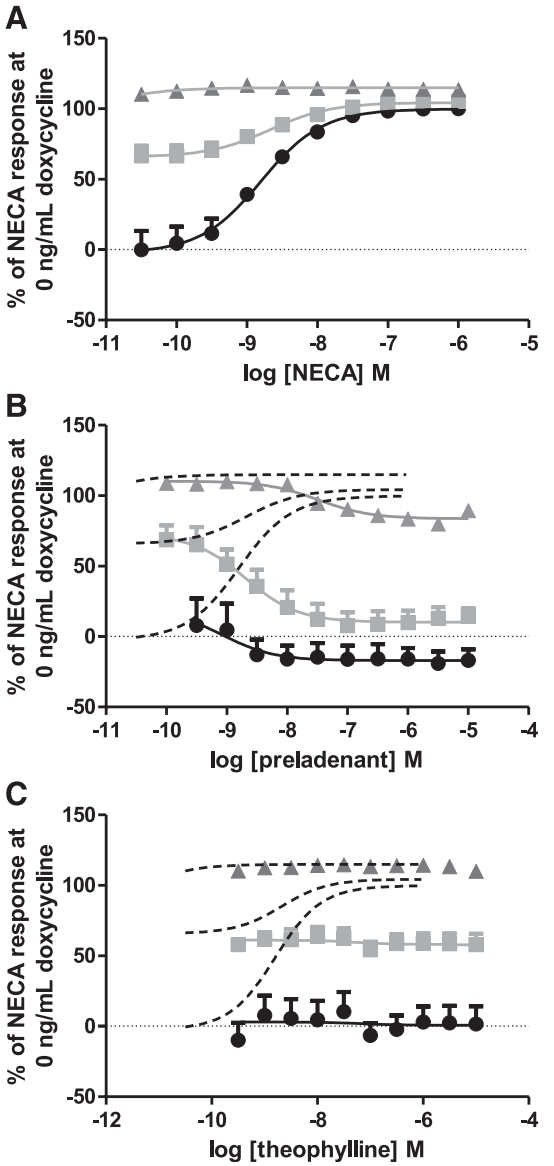

Fig. 4. Functional pharmacology of NECA, preladenant, and theophylline. Receptor expression was induced by the addition of 0 (filled circle), 0.3 (filled square), or 10 ng/ml (filled triangle) doxycycline for 16 hours before responses to NECA, preladenant, or theophylline were tested using a cAMP accumulation assay. (A) NECA acted as an agonist increasing cAMP production above basal, except at 10 ng/ml doxycycline where a response over basal could not be detected. (B) Preladenant acted as a full inverse agonist at 0 (filled circle) and 0.3 ng/ml (filled square) doxycycline but acted as a partial inverse agonist in situations with higher receptor expression levels (10 ng/ml doxycycline; filled triangle). NECA response is shown as a dotted line to allow comparison with agonist response. (C) Theophylline appeared to have no effect on basal cAMP concentrations at all receptor expression levels tested [0 (filled circle), 0.3 (filled square) and 10 ng/ml (filled triangle) doxycycline]. NECA response is shown as a dotted line to allow comparison with agonist response. Data shown as mean ± S.E.M. of $n = 3$.

adenosine A_{2A} receptor "antagonists" preladenant and istradefylline were docked into the binding site of the structure determined in complex with ZM241385 (3PWH; Figs. 5B and 6A). Preladenant is shown bound in a similar conformation to ZM241385; the triazolotriazine core and attached furan ring system both hydrogen-bond to $N253^{6.55}$. The aryl piperidine substituent of preladenant, while chemically distinct from the phenolic substituent of ZM241385, occupies the similar cleft between TM domains 1 and 7 (Fig. 6A). Due to its bulk, preladenant is expected to extend some way outside of the agonist-binding pocket as defined by the NECA-bound crystal structure (2YDV); furthermore, the furan ring sits in a similar position to that of ZM241385, sterically preventing the inward movement of $H250^{6.52}$. This pose clearly explains why it shows robust inverse agonist activity. For the placement of istradefylline in the binding site, previous SDM experiments

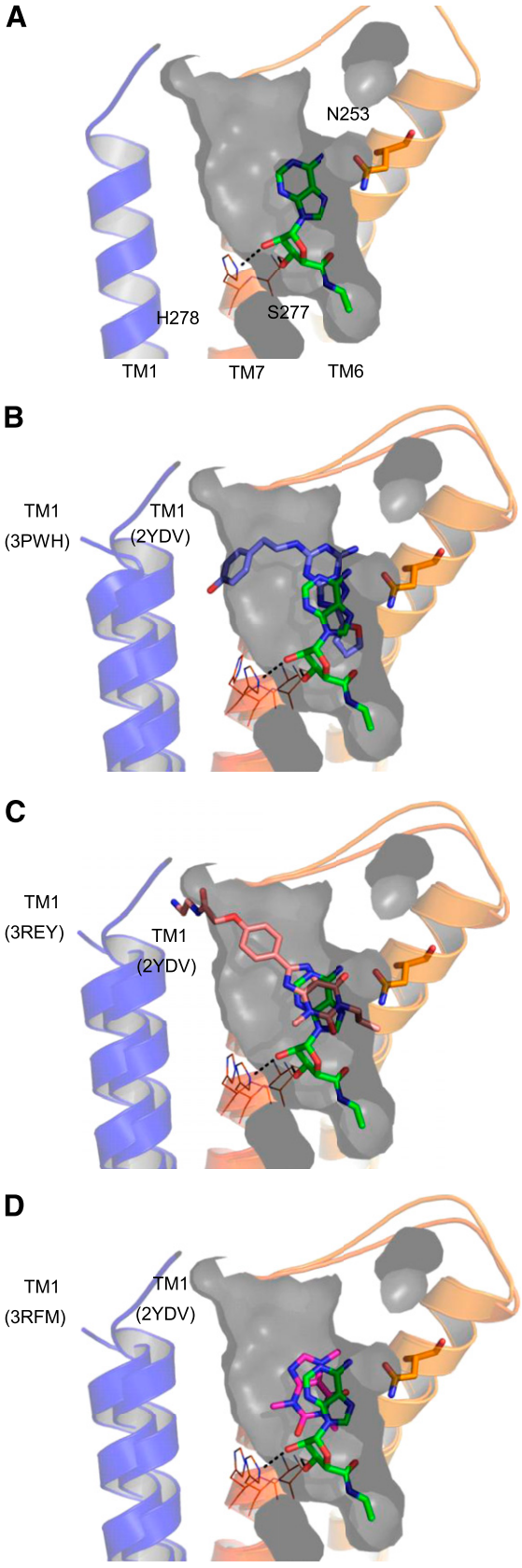

Fig. 5. Crystal structures of agonist and inverse agonists. (A) Crystal structure (2YDV) of NECA (green stick) bound to GL31. TM domains 2, 3, 4, and 5 have been removed for clarity. The gray shaded region highlights the extent of agonist binding pocket within the crystal structure. (B) ZM241385 (purple stick) co-crystal structure (3PWH) and (C) XAC (salmon stick) co-crystal structure (3REY) overlaid the NECA co-crystal structure 2YDV. In the inactive state, crystal structures TM1 is significantly moved outward compared with the NECA-bound structure. ZM241385 and XAC do not fully fit into the binding pocket defined in the agonist crystal structure. (D) The co-crystal structure of caffeine (pink stick) (3RFM) reveals that, due to its smaller size caffeine, can be accommodated in the agonist binding pocket.

show that istradefylline binding is less affected by an alanine mutation of either $I66^{2.64}$ or $Y271^{7.36}$ than by the effect on both XAC and ZM241385 (Zhukov et al., 2011). Thus, the SDM-guided docking of istradefylline shows (similar to caffeine) its carbonyl oxygen from C6 forming a hydrogen bond to $N253^{6.55}$; the vector of the ligand placement also points directly up toward the extracellular surface but is crucially still contained within the binding site surface defined by the NECA-bound agonist structure (2YDV; Fig. 6C), rationalizing the neutral antagonist profile observed.

Conversely, we sought to understand the potential interaction of NECA with the inactive conformation based on known structure (3PWH; Fig. 6C). While NECA can fully fit into the inactive state binding site, the significant movements of TM3 and TM7 (described in Dore et al., 2011) mean that the hydrogen bonds from $H278^{7.43}$ and $T88^{3.36}$ to the ligand are lost. The loss of two hydrogen bonds (each contributing in the range of 2–10 kcal/mol) would significantly reduce the affinity of NECA at the inactive state StaR compared with the active state StaR. The glide XP dockings of NECA in active and inactive states gave values of −11.0 and −6.2 respectively, emphasizing the preference for NECA at the active state. Glide XP dockings were also performed for istradefylline, caffeine, and theophylline at active- (2YDV) and inactive- (3PWH) state structures. Istradefylline showed a slight preference for binding to the inactive state (−4.5 in active structure; −6.5 in inactive structure), whereas caffeine and theophylline had little or no preference (caffeine: −5.6 at both active and inactive structures; theophylline: −6.4 at active-state and −6.9 at inactive-state). These findings predict istradefylline is a partial inverse agonist, and caffeine and theophylline are neutral antagonists.

Discussion

To facilitate crystallization, GPCRs have been successfully engineered to isolate either active or inactive conformations using StaR technology (Dore et al., 2011; Lebon et al., 2011b). This process identifies point mutations that stabilize the TM domain helices into or toward either the active or inactive state of the receptor. Here we have used binding affinities of ligands at adenosine A_{2A} receptors progressively stabilized into both inactive and active states to predict their molecular efficacy. Affinity ratios were then qualitatively compared with data generated using a functional cAMP assay at different levels of constitutive activity.

Ligands can display a wide spectrum of efficacies; they can act as full or partial agonists, appear silent (neutral antagonist) or display partial to full inverse agonism. The two-state model of receptor activation (Leff, 1995) ascribes ligand efficacy as a ratio of its affinity for the inactive (R) and active (R*) receptor states; agonists have higher affinity for R*, inverse agonists have higher affinity for R, and neutral antagonists do not select

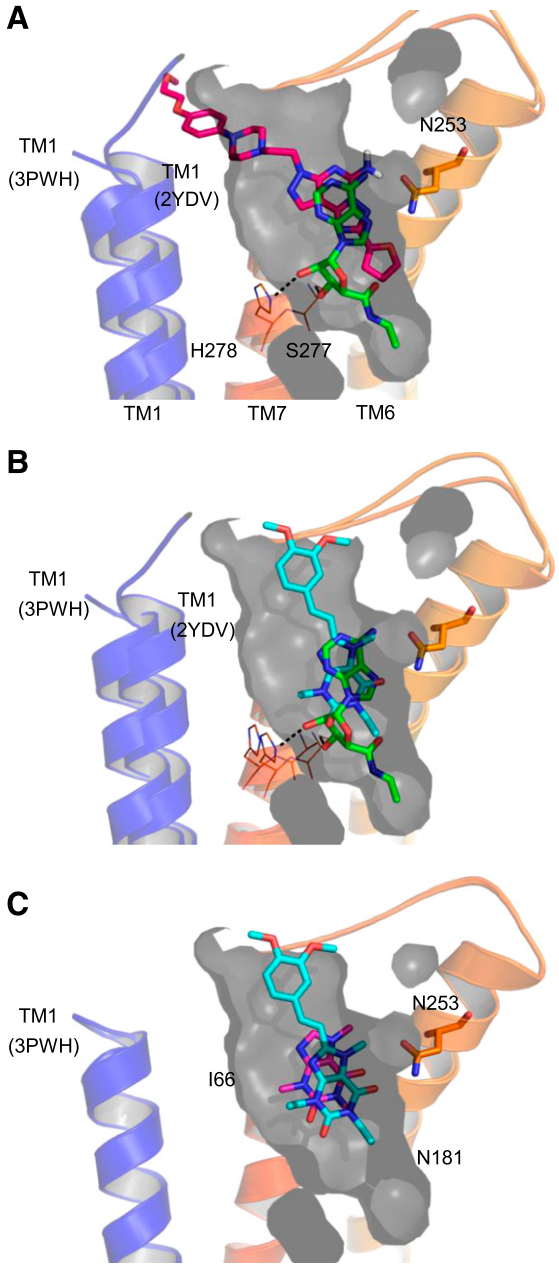

Fig. 6. Data-based docking of full and partial inverse agonists into the ZM241385 co-crystal structure. (A) Optimized preladenant (rose stick) docking based on BPM and pharmacologic data suggest that preladenant cannot fit within the agonist pocket (agonist pocket extracted from 2YDV shown in gray; NECA shown in green). (B) In contrast, istradefylline (cyan stick) is expected to fit vertically into the agonist-binding pocket in a similar fashion to caffeine (pink stick) (C).

between conformations. Although the two-state model is likely to be oversimplistic in describing GPCR pharmacology (i.e., it does not account for multiple conformations that exist between inactive/fully active receptors or for differences in activation states that result in biased agonism), it is extremely useful conceptually, describing the interactions of many GPCR ligands (Canals et al., 2012).

The data generated herein appears to be accommodated approximately within the two-state mechanism. The prototypical adenosine receptor agonist, NECA, displays significantly lower affinity at the inactive state A_{2A} receptor; the "antagonists" ZM241385, preladenant, SCH58261, and XAC bind with higher affinity to the inactive state (i.e., act as inverse agonists). Istradefylline, caffeine, and theophylline bind with similar affinities to both inactive and active states and would be defined as neutral antagonists.

We have previously demonstrated that adenosine A_{2A} receptor number and constitutive activity can be titrated using an inducible expression system (Lebon et al., 2011b). By optimizing the levels of induction, a system was created allowing measurement of agonist and inverse agonist responses (Fig. 3). We confirmed that affinity ratios correlated with efficacy in vitro; ZM241385, preladenant, SCH58261, and XAC acted as inverse agonists, and NECA acted as an agonist in the cAMP assay. Based on binding studies, istradefylline, caffeine and theophylline were predicted to act as neutral antagonists; this was verified in the functional assays where all three compounds displayed essentially neutral antagonism, although caffeine did display very weak partial inverse agonist efficacy (Fig. 4; Supplemental Fig. 1).

Measuring affinity constants for isolated GPCR conformations is not trivial; functional effects depend not only on efficacy but on other factors, such as receptor expression and signal amplification between receptor and endpoint measured. At low levels of receptor expression, NECA acts as an agonist of the adenosine A_{2A} receptor; however, when receptor density is increased, there is a point at which constitutive activity becomes so great that NECA can no longer elicit a response above basal (due to the maximal system response being reached; Fig. 3B). For the inverse agonists preladenant, ZM241385, SCH58261, and XAC, responses could only be measured in a system where there was sufficient basal activity to allow a "window" for reversal; if receptor density is further increased, it reaches a point where these ligands appear to act as partial inverse agonists (Fig. 4; Supplemental Fig. 1).

Using the crystal structures of both the active-state and inactive-state (Dore et al., 2011; Lebon et al., 2011b) adenosine A_{2A} receptor, we sought to rationalize the differences in pharmacology of the ligands tested in this study. The change in shape and size of the binding pocket upon agonist binding is marked (Dore et al., 2011; Lebon et al., 2011b), in effect yielding two different binding sites; the discrimination between the two sites dictates ligand pharmacology. By overlaying the agonist-binding site (Lebon et al., 2011b) onto the caffeine co-crystal structure, caffeine was shown to fit equally well into active- and inactive-state binding sites, functioning as a neutral antagonist. However, when similar overlay analyses were performed for ZM241385 and XAC, it became clear these ligands cannot be accommodated in the agonist-binding site, neither deep within the TM region (adjacent to $H250^{6.52}$) nor at the extracellular face. These observations explain why these compounds display a clear preference to bind to the inactive state of the receptor and hence function as inverse agonists. While NECA could fit into both active and inactive state structures, the loss of two hydrogen bonds in the inactive state would rationalize the significant reduction in affinity of NECA seen at the inactive state StaR. In the absence of co-crystal structures, we used a "reverse pharmacology" approach to help build models to predict istradefylline and preladenant binding to the adenosine A_{2A} receptor. Results of previous biophysical mapping/site-directed mutagenesis studies (Zhukov et al., 2011) indicated that istradefylline binding is insensitive to mutation of $I66^{2.64}$ or $Y271^{7.36}$ and hence binds deeper in the

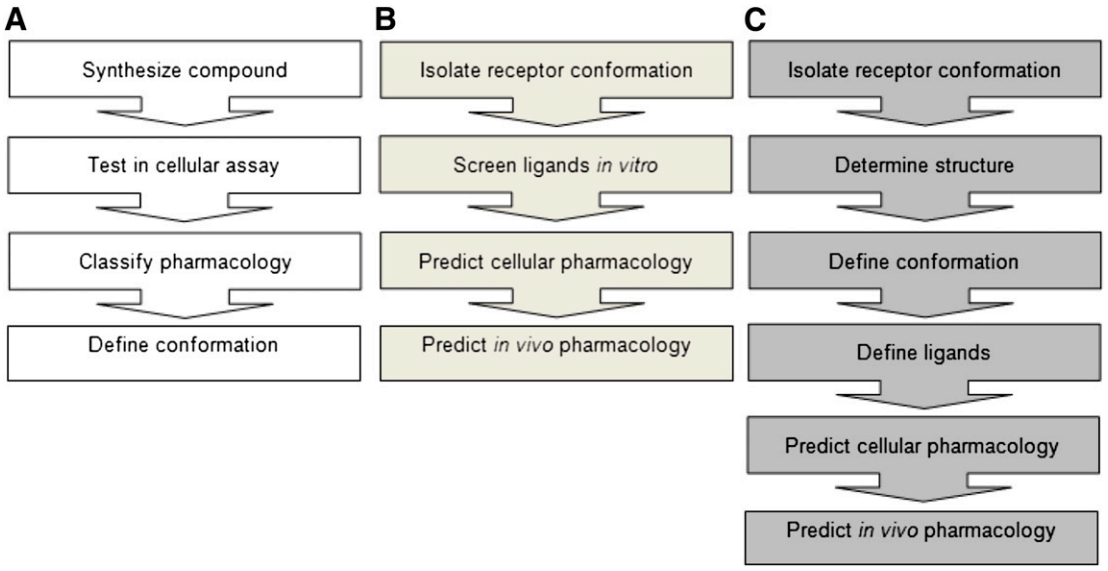

Fig. 7. The concept of reverse pharmacology. Comparison of (A) traditional and (B and C) novel approaches to GPCR pharmacology using StaR technology. By using isolated receptor conformations, it is possible to (B) screen ligands by in vitro binding to identify compounds that bind preferentially to a given conformation or (C) solve the structure of a defined conformation and de novo design, or screen in silico for ligands that bind to that conformation. In each case, the selectivity for the given conformation defines the pharmacology.

receptor than ZM241385 and XAC, but in a similar fashion to caffeine. The docking mode suggests istradefylline extends perpendicular to the membrane but is equally able to be accommodated in active and inactive state binding pocket. Thus, both affinity data and the docking mode predict for istradefylline to display neutral antagonism, a profile confirmed in functional analysis.

A similar approach was taken for predicting the binding mode of preladenant. Due to their chemical similarity, preladenant is predicted to bind in a mode similar to that of ZM241385, with the triazolotriazine core and furan ring forming H-bonding interactions with $N253^{6.55}$. As for ZM241385, the position of the furan ring is predicted to sterically prevent inward movement of $H250^{6.52}$, which is seen upon receptor activation. In addition, due to its increased bulk, the arylpiperidine moiety of preladenant is expected to extend even further than ZM241385 or XAC, beyond the extracellular-facing surface of the agonist-binding site (Fig. 6, A and B); these observations explain why preladenant has such low affinity for the active-state receptor and displays such robust inverse-agonist behavior.

Interestingly, the affinity of preladenant for the active state of the receptor compared with the wild-type receptor is decreased by a greater extent (approximately 300-fold at GL31) than that of ZM241385 (30-fold at GL31), even though ZM241385 had higher affinity for the wild-type receptor. This is consistent with the extent of change in affinity at R and R*, governed by the way in which a compound binds. It stands to reason that bulkier ligands are less able to bind into the smaller binding site of the active state and therefore have much reduced affinity for the active state, displaying a preference for the more "open" inactive state of the receptor.

Adenosine A_{2A} "antagonists" have been tested as nondopaminergic therapies for the treatment of Parkinson's disease. They are thought to provide their anti-Parkinsonian benefits by regulating dopamine D_2 receptors and reducing the overactivity in the striatopallidal pathway (Pinna, 2009). Istradefylline was evaluated for efficacy in the treatment of Parkinson's disease through to phase III clinical trials, but it was given a nonapprovable letter from the FDA (Pinna, 2009). Results suggested that istradefylline was well tolerated but did not appear to have sufficient efficacy, either alone or as an adjunctive therapy (Pinna, 2009). Preladenant demonstrated good efficacy in phase IIa trials in patients with moderate-to-severe Parkinson's disease when administered in conjunction with levodopa therapy (Salamone, 2010) and has entered into phase III clinical trials, both as an adjunct to levodopa and as monotherapy. Direct comparisons of clinical efficacy are not easy (and of course, other factors, such as pharmacokinetic properties, are important), but istradefylline and preladenant exert demonstrably different pharmacology at the adenosine A_{2A} receptor. Given some reports suggesting that the adenosine A_{2A} receptor may be constitutively active in endogenous systems (Ibrisimovic et al., 2012) and even in vivo (Le Moine et al., 1997), inverse agonist activity may be required for greater efficacy in regulation of dopamine D_2 receptors and the treatment of Parkinson's disease.

Here we demonstrated that, by determining ligand affinities at the adenosine A_{2A} receptor isolated at both active and inactive states, it is possible to make qualitative, system-independent assessment of ligand pharmacology. This could help distinguish neutral antagonists from inverse agonists, which is hard to do functionally in vitro where there is a low level of constitutive activity in the system [(R)>>(R*)], as inverse agonists will be indistinguishable from neutral antagonists. This is highly relevant; inverse agonists may be therapeutically useful in the treatment of diseases linked with constitutive receptor activation, such as severe Jansen-type metaphyseal chondrodysplasia (Schipani et al., 1995), fragile X-linked disorder (Ronesi et al., 2012), or autoimmune diseases (de Ligt et al., 2000). Furthermore, we demonstrated that analysis of putative docking modes into the active and inactive state crystal structures supports the functional observations and permits an in silico assessment of ligand pharmacology. The concept of predicting whether a compound

has a propensity to behave as an agonist, neutral antagonist, or inverse agonist in a cellular or in vivo setting is a potentially powerful tool for researchers (Fig. 7).

Authorship Contributions

Participated in research design: Bennett, Marshall, Langmead, Weir.

Conducted experiments: Bennett.

Contributed new reagents or analytic tools: Bennett, Lebon, Tate.

Performed data analysis: Bennett, Tehan, Langmead.

Wrote or contributed to the writing of the manuscript: Bennett, Langmead, Tehan, Tate, Marshall, Weir.

References

Bennett K, Guillaume L, Tehan B, Tate C, and Langmead C (2011) Investigation into the pharmacology of the adenosine A_{2A} receptor stabilised in an active-state conformation. *Proceedings of the British Pharmacological Society*; 2011 Dec 13–15; London, UK.

Canals M, Lane JR, Wen A, Scammells PJ, Sexton PM, and Christopoulos A (2012) A Monod-Wyman-Changeux mechanism can explain G protein-coupled receptor (GPCR) allosteric modulation. *J Biol Chem* **287**:650–659.

Congreve M, Andrews SP, Doré AS, Hollenstein K, Hurrell E, Langmead CJ, Mason JS, Ng IW, Tehan B, and Zhukov A et al. (2012) Discovery of 1,2,4-triazine derivatives as adenosine A(2A) antagonists using structure based drug design. *J Med Chem* **55**:1898–1903.

De Lean A, Stadel JM, and Lefkowitz RJ (1980) A ternary complex model explains the agonist-specific binding properties of the adenylate cyclase-coupled beta-adrenergic receptor. *J Biol Chem* **255**:7108–7117.

de Ligt RA, Kourounakis AP, and IJzerman AP (2000) Inverse agonism at G protein-coupled receptors: (patho)physiological relevance and implications for drug discovery. *Br J Pharmacol* **130**:1–12.

Doré AS, Robertson N, Errey JC, Ng I, Hollenstein K, Tehan B, Hurrell E, Bennett K, Congreve M, and Magnani F et al. (2011) Structure of the adenosine A(2A) receptor in complex with ZM241385 and the xanthines XAC and caffeine. *Structure* **19**: 1283–1293.

Foord SM, Bonner TI, Neubig RR, Rosser EM, Pin JP, Davenport AP, Spedding M, and Harmar AJ (2005) International Union of Pharmacology. XLVI. G protein-coupled receptor list. *Pharmacol Rev* **57**:279–288.

Fredholm BB, Johansson S, and Wang YQ (2011) Adenosine and the regulation of metabolism and body temperature. *Adv Pharmacol* **61**:77–94.

Guo D, Mulder-Krieger T, Ijzerman AP, and Heitman LH (2012) Functional efficacy of adenosine A(2A) receptor agonists is positively correlated to their receptor residence time. *Br J Pharmacol* **166**:1846–1859.

Ibrisimovic E, Drobny H, Yang Q, Hofer T, Boehm S, Nanoff C, and Schicker K (2012) Constitutive activity of the A(2A) adenosine receptor and compartmentalised cyclic AMP signalling fine-tune noradrenaline release. *Purinergic Signal* **8**:677–692.

Katritch V, Cherezov V, and Stevens RC (2012) Diversity and modularity of G protein-coupled receptor structures. *Trends Pharmacol Sci* **33**:17–27.

Kent RS, De Lean A, and Lefkowitz RJ (1980) A quantitative analysis of beta-adrenergic receptor interactions: resolution of high and low affinity states of the receptor by computer modeling of ligand binding data. *Mol Pharmacol* **17**:14–23.

Langmead CJ, Andrews SP, Congreve M, Errey JC, Hurrell E, Marshall FH, Mason JS, Richardson CM, Robertson N, and Zhukov A et al. (2012) Identification of novel adenosine A(2A) receptor antagonists by virtual screening. *J Med Chem* **55**: 1904–1909.

Le Moine C, Svenningsson P, Fredholm BB, and Bloch B (1997) Dopamine-adenosine interactions in the striatum and the globus pallidus: inhibition of striatopallidal neurons through either D2 or A2A receptors enhances D1 receptor-mediated effects on c-fos expression. *J Neurosci* **17**:8038–8048.

Lebon G, Bennett K, Jazayeri A, and Tate CG (2011a) Thermostabilisation of an agonist-bound conformation of the human adenosine A(2A) receptor. *J Mol Biol* **409**:298–310.

Lebon G, Warne T, Edwards PC, Bennett K, Langmead CJ, Leslie AG, and Tate CG (2011b) Agonist-bound adenosine A2A receptor structures reveal common features of GPCR activation. *Nature* **474**:521–525.

Leff P (1995) The two-state model of receptor activation. *Trends Pharmacol Sci* **16**: 89–97.

Overington JP, Al-Lazikani B, and Hopkins AL (2006) How many drug targets are there? *Nat Rev Drug Discov* **5**:993–996.

Perez DM, Hwa J, Gaivin R, Mathur M, Brown F, and Graham RM (1996) Constitutive activation of a single effector pathway: evidence for multiple activation states of a G protein-coupled receptor. *Mol Pharmacol* **49**:112–122.

Pinna A (2009) Novel investigational adenosine A2A receptor antagonists for Parkinson's disease. *Expert Opin Investig Drugs* **18**:1619–1631.

Rieger JM, Brown ML, Sullivan GW, Linden J, and Macdonald TL (2001) Design, synthesis, and evaluation of novel A2A adenosine receptor agonists. *J Med Chem* **44**:531–539.

Robertson N, Jazayeri A, Errey J, Baig A, Hurrell E, Zhukov A, Langmead CJ, Weir M, and Marshall FH (2011) The properties of thermostabilised G protein-coupled receptors (StaRs) and their use in drug discovery. *Neuropharmacology* **60**:36–44.

Ronesi JA, Collins KA, Hays SA, Tsai NP, Guo W, Birnbaum SG, Hu JH, Worley PF, Gibson JR, and Huber KM (2012) Disrupted Homer scaffolds mediate abnormal mGluR5 function in a mouse model of fragile X syndrome. *Nat Neurosci* **15**: 431–440.

Salamone JD (2010) Preladenant, a novel adenosine A(2A) receptor antagonist for the potential treatment of parkinsonism and other disorders. *IDrugs* **13**:723–731.

Samama P, Cotecchia S, Costa T, and Lefkowitz RJ (1993) A mutation-induced activated state of the beta 2-adrenergic receptor. Extending the ternary complex model. *J Biol Chem* **268**:4625–4636.

Schipani E, Kruse K, and Jüppner H (1995) A constitutively active mutant PTH-PTHrP receptor in Jansen-type metaphyseal chondrodysplasia. *Science* **268**: 98–100.

Shibata Y, White JF, Serrano-Vega MJ, Magnani F, Aloia AL, Grisshammer R, and Tate CG (2009) Thermostabilization of the neurotensin receptor NTS1. *J Mol Biol* **390**:262–277.

Strange PG (2000) Agonist binding to G-protein coupled receptors. *Br J Pharmacol* **129**:820–821.

Sullivan GW, Rieger JM, Scheld WM, Macdonald TL, and Linden J (2001) Cyclic AMP-dependent inhibition of human neutrophil oxidative activity by substituted 2-propynylcyclohexyl adenosine A(2A) receptor agonists. *Br J Pharmacol* **132**: 1017–1026.

Tate CG and Schertler GF (2009) Engineering G protein-coupled receptors to facilitate their structure determination. *Curr Opin Struct Biol* **19**:386–395.

Warne T, Serrano-Vega MJ, Baker JG, Moukhametzianov R, Edwards PC, Henderson R, Leslie AG, Tate CG, and Schertler GF (2008) Structure of a beta1-adrenergic G-protein-coupled receptor. *Nature* **454**:486–491.

Zhukov A, Andrews SP, Errey JC, Robertson N, Tehan B, Mason JS, Marshall FH, Weir M, and Congreve M (2011) Biophysical mapping of the adenosine A2A receptor. *J Med Chem* **54**:4312–4323.

Address correspondence to: Dr. Fiona H. Marshall, Heptares Therapeutics Ltd, Biopark, Broadwater Road, Welwyn Garden City, Hertfordshire AL7 3AX. E-mail: fiona.marshall@heptares.com